



FULL LENGTH ARTICLE

ROS and Lipid Droplet accumulation induced by high glucose exposure in healthy colon and Colorectal Cancer Stem Cells



Luca Tirinato ^{a,b,c,*},¹, Francesca Pagliari ^{a,d,1},
Simone Di Franco ^e, Elisa Sogne ^d, Maria Grazia Marafioti ^a,
Jeanette Jansen ^{a,f}, Andrea Falqui ^d, Matilde Todaro ^g,
Patrizio Candeloro ^c, Carlo Liberale ^d, Joao Seco ^{a,f},
Giorgio Stassi ^e, Enzo Di Fabrizio ^{b,**}

^a Biomedical Physics in Radiation Oncology, DKFZ (German Cancer Research Center), 69120 Heidelberg, Germany

^b Physical Science and Engineering (PSE) Division, King Abdullah University of Science and Technology (KAUST), Thuwal, Saudi Arabia

^c Department of Experimental and Clinical Medicine, University "Magna Graecia" of Catanzaro, 88100 Loc. Germaneto, Catanzaro, Italy

^d Biological and Environmental Sciences and Engineering (BESE) Division, King Abdullah University of Science and Technology (KAUST), Thuwal 23955-6900, Saudi Arabia

^e Cellular and Molecular Pathophysiology Laboratory, Department of Surgical, Oncological and Stomatological Sciences, University of Palermo, Palermo, Italy

^f Ruprecht Karls University Heidelberg, Department of Physics, 69120 Heidelberg, Germany

^g Department of Health Promotion, Mother and Child Care, Internal Medicine and Medical Specialties (PROMISE), University of Palermo, Palermo, Italy

Received 3 July 2019; accepted 12 September 2019

Available online 25 September 2019

KEYWORDS

Cholesterol metabolism;
Colorectal cancer stem cells;
Fatty acid

Abstract Lipid Droplets (LDs) are emerging as crucial players in colon cancer development and maintenance. Their expression has been associated with high tumorigenicity in Cancer Stem Cells (CSCs), so that they have been proposed as a new functional marker in Colorectal Cancer Stem Cells (CR-CSCs). They are also indirectly involved in the modulation of the tumor microenvironment through the production of pro-inflammatory molecules. There is growing evidence that a possible connection between metabolic alterations and malignant

* Corresponding author. Biomedical Physics in Radiation Oncology, DKFZ (German Cancer Research Center), 69120 Heidelberg, Germany.

** Corresponding author.

E-mail address: tirinatomail@gmail.com (L. Tirinato).

Peer review under responsibility of Chongqing Medical University.

¹ These Authors contributed equally to the work.

metabolism;
High glucose;
Lipid droplets;
Oncogenes;
Oxidative stress;
PI3K-AKT

transformation exists, although the effects of nutrients, primarily glucose, on the CSC behavior are still mostly unexplored. Glucose is an essential fuel for cancer cells, and the connections with LDs in the healthy and CSC populations merit to be more deeply investigated. Here, we showed that a high glucose concentration activated the PI3K/AKT pathway and increased the expression of CD133 and CD44v6 CSC markers. Additionally, glucose was responsible for the increased amount of Reactive Oxygen Species (ROS) and LDs in both healthy and CR-CSC samples. We also investigated the gene modulations following the HG treatment and found out that the healthy cell gene profile was the most affected. Lastly, Atorvastatin, a lipid-lowering drug, induced the highest mortality on CR-CSCs without affecting the healthy counterpart.

Copyright © 2019, Chongqing Medical University. Production and hosting by Elsevier B.V. This is an open access article under the CC BY-NC-ND license (<http://creativecommons.org/licenses/by-nc-nd/4.0/>).

Introduction

The World Health Organization (WHO) guidelines recommend limiting the daily free sugar intake for children and adult at, if not lower, 10% of the total energy intake.¹ Despite being key sources of carbon and energy for cellular metabolism, epidemiological studies demonstrated that the excess of sugars, especially glucose, in diet leads to obesity,² higher risk of heart diseases³ and diabetes, including several related conditions, such as inflammation, high blood pressure and insulin resistance.⁴ Moreover, some studies report that an indirect link exists between sugar-related diseases and an increasing risk of cancer.^{5,6} However, in 2012 the European Prospective Investigation into Cancer and Nutrition (EPIC) study has instead shown a direct correlation between high dietary sugar intake and a higher risk of developing cancer.⁷

The exact mechanisms by which glucose might favor cancer development are currently not fully understood. Nowadays, glucose and lipid metabolic alterations have been proposed as hallmarks of cancer, since several studies are highlighting their involvement in malignant transformation and cancer growth.^{8,9} Glucose is considered an essential nutrient for cells, especially for cancer cells in which the aerobic glycolysis is believed to be the favorite pathway for producing ATP (the Warburg effect) to sustain rapid growth.⁵ However, recent reports demonstrated that cancer cells can also rely on the tricarboxylic acid (TCA) cycle, which produces larger amounts of ATP through the oxidative phosphorylation (OXPHOS) and biosynthetic precursors of amino acids, lipids and nucleotides.¹⁰ Glucose metabolism produces ROS,⁶ and high glucose (HG) concentrations can induce *de novo* lipogenesis with free fatty acid (FA) and triacylglycerol (TAG) production.¹¹

Oxidative stress is considered one of the leading players in altered metabolic pathways. Healthy cells in normal conditions counteract oxidative stress by activating protective responses that can be not sufficient in stress conditions. Compelling evidence suggests that a pro-oxidant status might lead to inflammatory processes and consequently to diseases, such as diabetes and cancer.¹² Indeed, different types of cancer cells display high levels of oxidative stress, which seem to favor cancer cell pro-

liferation and migration, as well as resistance to treatments.¹³

Deregulated lipid metabolism in cancer includes the ability of malignant cells to preferentially synthesize and use the endogenous sources coupled with more efficient mechanisms to uptake the extracellular lipids.¹⁴ This behavior translates into a high rate of lipid metabolism that has been linked to carcinogenesis and metastasis.^{9,15} In particular, increased LD accumulation seem to be a common feature of several cancers, including colorectal cancer (CRC), where they are thought to act also as protective organelles against the toxicity due to excess of ROS and free lipids, energy suppliers and sites for synthesis of inflammatory mediators, thus favoring cell survival, aggressiveness and resistance to treatments.^{16–22} In this context, a small subpopulation of cells inside the tumor mass, called Cancer Stem Cells (CSCs), is considered to be the responsible for tumor initiation and progression, chemo- and radio-resistance, relapse and metastasis.²³ Therefore, LDs could participate in determining CSC features. Indeed, in some tumors, CSCs have been shown to have higher LD content and, recently, LDs have been proposed as a new functional marker in CR-CSCs.²⁴

The mechanisms behind such metabolic alterations in healthy and cancer tissues are the subject of intense study. Several oncogenic pathways result altered and, among them, the PI3/AKT/mTOR signaling cascade is one of the most investigated.²⁵

Collectively, these observations point out to an intriguing yet complex role of metabolic alterations in linking diabetes and obesity with cancer. Nevertheless, the effects of HG conditions on CSCs largely remain unexplored, while wider knowledge has been gained in the healthy counterpart. Based on these considerations, the present study aimed at investigating the responses to HG of healthy colon cells (HCCs) and CR-CSCs, in comparison with a normal glucose (NG) exposure. In particular, in our culture conditions, modulations of stemness markers and PI3/AKT protein expression were observed in CR-CSCs. Furthermore, HG triggered ROS increase and LD accumulation, as well as activation of genes related to lipid metabolism and tumorigenesis, more largely in HCCs than in CR-CSCs.

Finally, in an attempt to interfere with lipid synthesis pathways, the use of Atorvastatin alone in NG and HG or in combination with DGAT2 inhibitor (interfering with cholesterol and TAG synthesis respectively) in NG reduced significantly cell viability in comparison with Oxaliplatin, a conventional chemotherapy drug used for treating CRC. The present study may provide important implications in the study of glucose-related diseases, including diabetes and obesity, and contribute to our understanding of the initiation and maintenance processes in glucose-linked cancers.

Materials and methods

Ethics approval and consent to participate

All study procedures were approved by the Institutional Review Board of University of Palermo and King Abdullah University of Science and Technology. Cancer tissues were taken after written informed consent has been obtained. All research was performed in accordance with relevant guidelines and regulations.

Cell cultures

CCD841 CoN epithelial colon cells (HCCs) (ATCC CRL-1790) were cultured in Eagle's Minimum Essential Medium (ATCC; #30-2003) supplemented with 10% fetal bovine serum (FBS) (ATCC; 30-2020) and 1% (v/v) penicillin/streptomycin (Gibco; #15140122) in TC-treated flasks (Corning, Lowell, MA) and passaged using 1X Tryple Express Enzyme (Thermo Fisher Scientific; #12604039).

Colorectal cancer (CRC) tissues were obtained following surgical resection, under the ethical standards of the institutional committee of the University of Palermo. Cancer specimens were mechanically and enzymatically digested using collagenase and hyaluronidase shaking for 1 hour at 37 °C. Digests were cultured in ultralow adhesion flasks (Corning; #CLS3815) to enrich the cell culture in CSCs, with a serum-free Advanced DMEM/F12 medium (Thermo Fisher Scientific; #12634010), supplemented with 10 mM HEPES (Gibco; #15630080), 1 mM N-acetyl-L-cysteine (Sigma Aldrich; #A9165), 1X N2 supplement (Thermo Fisher Scientific; #17502048), 1X B-27 (Thermo Fisher Scientific; #12587010), 10 mM Nicotinamide (Sigma Aldrich; #N0636); 20 ng/mL of recombinant human Epidermal Growth Factor (EGF) and 10 ng/mL of human recombinant basic Fibroblast Growth Factor (bFGF) (both from Peprotech; #AF-100-15 and #100-18C, respectively). Following isolation protocol, we evaluated the expression of CD133/CD44v6/CD166 CSC markers by FACS.²⁶ Each CR-CSC line has been used to test its tumorigenic potential by subcutaneously injecting them into NOD/SCID mice. Cells were maintained at 37 °C in a 5% CO₂ humidified incubator. Cancer spheroids were expanded *in vitro* for several passages, by enzymatic and mechanical dissociation. Cancer spheroids grown under these culture conditions were routinely screened by FACS for the expression of CR-CSC markers.^{27,28}

Glucose supplementation

For the normal glucose (NG) condition, cells were cultured in their own complete media without adding D-Glucose (glucose) (Gibco; #A2494001), while, in order to mimic a very high glucose condition, cells were maintained in their media supplemented with a final concentration of 50 mM glucose (HG) for 72 hrs.

CR-CSC marker analysis

Cells were dissociated, harvested, washed twice in Phosphate Buffer Solution (PBS) 1X (Thermo Fisher Scientific; #10010023) and stained with conjugated antibodies CD44v6-APC (2F10, mouse IgG1) (R&D systems; #FAB3660A), CD133/2-APC (293C3-APC) (Miltenyi Biotec; #130-090-854), or corresponding isotype-matched control (IMC) CD3e-APC (UCHT1, mouse IgG1) (R&D systems; #FAB100A). Stained cells were analyzed using the Accuri C6 (Becton Dickinson) flow cytometer. Analysis of protein expression levels was performed using FlowJo software (ver. 10).

Western blot

Protein lysates of glucose-treated and –untreated CR-CSCs were obtained by treating cells with ice-cold buffer containing 10 mM Tris-HCl (Sigma Aldrich; #10812846001), 50 mM NaCl (Sigma Aldrich, #S3014), 30 mM sodium pyruvate (Sigma Aldrich; #P8574), 50 mM NaF (Sigma Aldrich; #215309), 5 μM ZnCl₂ (Sigma Aldrich; #229997), 1% Triton (Bio-Rad; #1610407), protease inhibitor cocktail (Sigma Aldrich; #P8340), phosphatase inhibitor cocktail 2 and 3 (Sigma Aldrich; #P5726 and #P0044 respectively), 0.1 mM sodium orthovanadate (Sigma Aldrich; #450243), 10 mM sodium butyrate (Sigma Aldrich; #B5887) and 1 mM PMSF (Sigma Aldrich; #93482). Proteins were then loaded in a SDS-PAGE gel and blotted on a nitrocellulose membrane. Membranes were exposed to a blocking solution made by PBS 0.1% Tween 20 (Sigma Aldrich; #P1379) and 5% non-fat dry milk (Sigma Aldrich; #M7409) for 1 hour at room temperature, and then incubated overnight at 4 °C with primary antibodies specific for PI3K p110α (C73F8, rabbit IgG) (Cell Signaling Technologies; #4249), phospho-AKT (Ser473) XP (D9E, rabbit, IgG) (Cell Signaling Technologies; #4060), AKT (rabbit polyclonal) (Cell Signaling Technologies; #9272). β-actin (8H10D10, mouse) (Cell Signaling Technologies; #3700) was used as loading control. Primary antibodies were detected by incubating the membranes with secondary antibodies, anti-mouse or anti-rabbit, HRP-conjugated (goat H + L) (Thermo Fisher Scientific) for 1 hour at room temperature. Luminescence signal was revealed using SuperSignal™ West Dura Extended Duration Substrate (Thermo Fisher Scientific) and Amersham imager 600 (GE Healthcare). Protein levels were calculated by densitometric analysis using ImageJ software.

ROS and LD quantification

Intracellular general ROS content was measured by using freshly prepared chloromethyl-dichlorodihydrofluorescein diacetate (CM-H₂DCFDA) (Thermo Fisher Scientific;

#C6827) dye resuspended in anhydrous Dimethyl Sulfoxide (DMSO) (Thermo Fisher Scientific; #D12345) according to manufacturer's instructions. LD content was assessed by staining with LD540.²⁴ 10^6 cells were seeded in T75 flasks with or without 50 mM glucose and analyzed after 72 hours (hrs). After treatment, HCCs and CR-CSCs were centrifuged, resuspended in PBS 1X and counted using a Bürker counting chamber (BLAUBRAND) by trypan blue (Thermo Fisher Scientific; #15250061) exclusion method. Then, 5×10^5 live cells were incubated either with 3.5 μ M CM-H2DCFDA in pre-warmed Hanks' balanced salt solution (HBSS) (Thermo Fisher Scientific; #14025050) for 20 minutes (min) at 37 °C or 1:5000 LD540 in PBS 1X for 10 min at room temperature, in the dark. After washing with PBS 1X, cells were acquired on a FACSCanto II flow cytometer (BD Biosciences) using a 488 nm laser for the excitation of both dyes. The median fluorescence intensity was analyzed using FlowJo software (ver. 10).

Confocal microscopy

To image LDs after 72 hrs of HG treatment, HCCs and CR-CSCs were stained with LD540 1:5000 in PBS 1X for 10 min in the dark and, after 3 washes in PBS 1X, nuclei were counterstained with NucBlue™ Live ReadyProbes™ Reagent (Thermo Fisher Scientific; #R37605) and, immediately imaged under the microscope. Fluorescence images were collected with both a Zeiss LSM710 and a Leica SP5 confocal-laser-scanning microscopies, equipped with a 63X i-Plan Apochromat (numerical aperture 1.40) and a 63X HCX PL APO (numerical aperture 1.4) oil immersion objectives, respectively.

The Avizo 9.3 image reconstruction software was used for processing the confocal image stacks. Avizo's Noise Reduction Median algorithms were applied for background noise reduction. Feature extraction and reconstruction (nuclei, LDs and cell membranes) were performed with semi-automated image segmentation.

RNA extraction and Real-Time qPCR

After 72 hrs in NG or HG, 10^6 HCCs or CR-CSCs were processed to extract total RNA using the High Pure RNA isolation kit (Roche; #11828665001) and 1 μ g RNA was retro-transcribed in cDNAs by means of the RT2 First Strand Kit (Qiagen; #330404), according to the manufacturer's instructions, in a C1000 Touch™ Thermal Cycler (Bio-Rad). After that, cDNAs were mixed with RT2 SYBR® Green qPCR Mastermixes (Qiagen; #330529) and aliquoted into 96-well RT2 Profiler PCR Arrays (Qiagen), for the simultaneous detection of gene panels related to Fatty Acid Metabolism (#PAHS-007Z), Lipoprotein Signaling and Cholesterol Metabolism (#PAHS-080Z), Oxidative Stress (#PAHS-065Z) and Oncogenes and Tumor Suppressor Genes (#PAHS-502Z), in a ABI 7900HT Real-Time PCR System (RT-qPCR) (Thermo Fisher Scientific). Data analysis of triplicated plates was performed using the software available at the Data Analysis Center (<http://www.qiagen.com/geneglobe>, Qiagen) and a 2-fold change was chosen as a cut-off. Normalization of CT

values was done on β -actin (housekeeping gene) expression and $2(-\Delta\Delta CT)$ method was used to calculate the fold changes of treated (HG) versus untreated (NG) samples.

Drug treatments and propidium iodide staining

HCCs and CR-CSCs were seeded (3×10^5 cells/well) in 24-well plates (Corning; #CLS3527) in NG media for 24, 48 and 72 hrs, supplemented with either Oxaliplatin (Sigma Aldrich; #O9512) or Atorvastatin (Sigma Aldrich; #PZ0001) or PF-06424439 (Sigma Aldrich; #PZ0233), used singularly (for HCCs and CR-CSCs) or in double combination (only for CR-CSCs). Moreover, CR-CSCs were also treated with the same drugs in HG for the same time points. Subsequently, cells were collected and stained with 2 μ g/mL Propidium Iodide (PI) (Sigma Aldrich; #P4864) in PBS 1X soon before the acquisition at the FACSCanto II cytometer, by using an excitation of 488 nm.

Statistical analysis

Survival results presented in the Fig. 7 were obtained using the "R2: Genomics Analysis and Visualization Platform (<http://r2.amc.nl>, <http://r2platform.com>)" and analyzed with a log-rank (Mantel–Cox) test and expressed as Kaplan–Meier survival curves.

All data have been run in triplicates and are expressed as means \pm SD. Statistical analyses have been performed by t-test or One-way ANOVA as indicated in the figure legends. Statistical significance was indicated as follow: $p \leq 0.05$ (*), $p \leq 0.01$ (**) and $p \leq 0.001$ (***). Only values with a significance ≤ 0.05 have been taken into consideration.

Results

CSC markers are upregulated by high glucose concentration

Four different CR-CSC cell lines, which grew *in vitro* as tumor organoids (Fig. 1a), have been cultured for 72 hrs in NG or HG concentration. We have previously demonstrated that CD133 is a cell surface molecule specifically expressed on CR-CSCs,²⁹ and that activation of PI3K/Akt pathway labels the metastatic CR-CSCs, identified for the expression of CD44v6.²⁷ Thus, to investigate the contribution of glucose in the regulation of cancer stemness, at the end of the incubation, CR-CSCs have been analyzed for the PI3K-AKT pathway activation and for the expression of CD133 and CD44v6, by Western blot and FACS, respectively. Our results showed that a 72 hrs time exposure to HG concentration was sufficient to hyperactivate the PI3K pathway, as demonstrated by the upregulated phosphorylation of AKT (p-AKT) (Fig. 1b). Given the role of PI3K/AKT pathway in cancer,³⁰ these findings suggested a putative role of glucose metabolism in the regulation of several aspects of CR-CSC behavior, including proliferation and survival. To ascertain the correlation between the activation of PI3K/AKT pathway and the establishment of a CSC phenotype, we

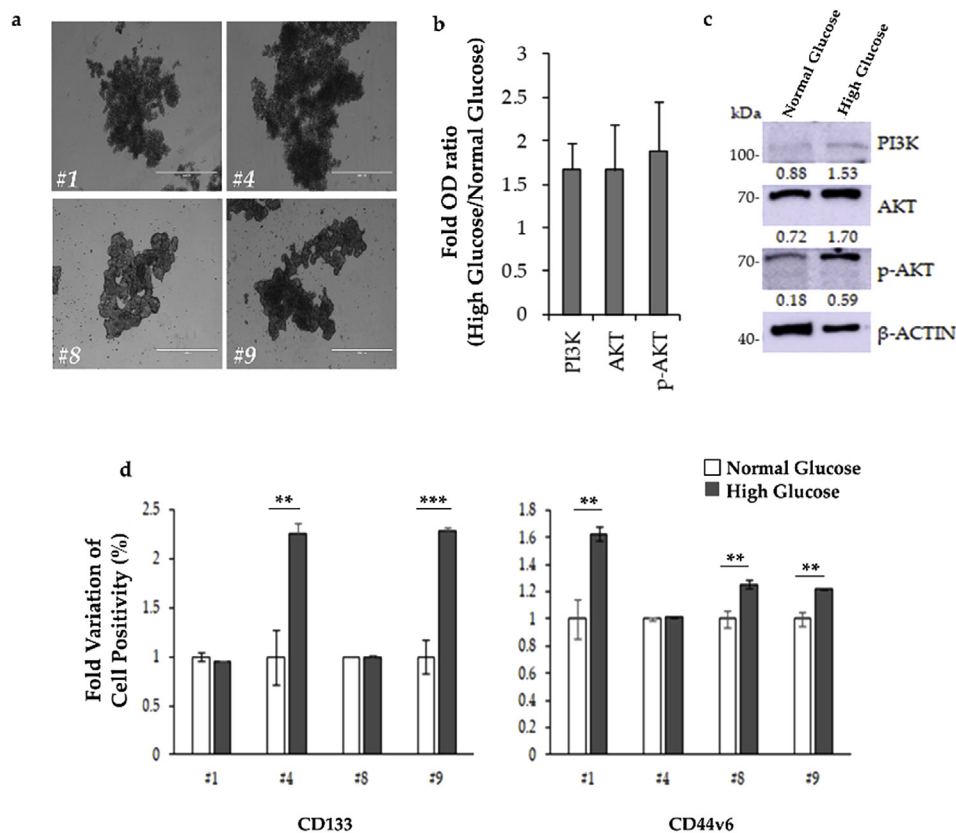


Figure 1 72 hrs in HG cell culture medium is sufficient to increase CSC markers in CR-CSCs. **a**) Primary CR-CSC spheroids (#1, #4, #8 and #9) were cultured in ultra-low adhesion flasks and morphology was assessed by phase-contrast microscopy (scale bar: 1000 μ m). **b**) Fold variation of protein expression in CR-CSCs treated with HG versus NG. Data are representative of 3 independent experiments performed with cells derived from 3 different CR-CSC lines. **c**) Representative Western blot of PI3K, phosphorylated (p-AKT) and total AKT in CR-CSC treated with HG or NG (#9 CR-CSC line is shown). β -Actin has been used as loading control. The uncropped blots are reported in [Supplementary Fig. 1](#). **d**) Fold variation of positivity for CD133 or CD44v6 in CR-CSCs treated as in (b and c), measured by FACS.

assessed the expression of both CD133 and CD44v6 CSC markers in all CSC lines, upon HG treatment. Interestingly, cells treated with HG medium showed significantly higher expression of CD133 (#4), CD44v6 (#1 and #8), or both cell surface markers (#9), compared to cells grown in control medium (Fig. 1c). In light of these results, we could speculate that constant and prolonged exposure to an increased amount of glucose in tumor context could dramatically affect cancer cell proliferation.

High glucose concentration increases the amount of lipid droplets and ROS

To assess whether HG induced oxidative status modification, HCCs and CR-CSCs were cultured in NG or HG media for 72 hrs. Fig. 2a shows that HG conditions induced a statistically significant increase of ROS both in HCCs and CR-CSCs, as assessed by using CM-H2DCFDA probe, a general oxidative stress indicator. In particular, HCCs showed approximately 40% (Fig. 2a left side) and CR-CSCs 12%

(Fig. 2a right side) increase in ROS, as compared with the respective controls.

Furthermore, the effect of HG condition on the LD modulation was also investigated. As shown in Figure 2, 72 hrs of 50 mM glucose treatment induced LD accumulation in HCCs (almost 30%) (Fig. 2b left side) and at a minor extent, but still significant, in CR-CSCs (9%) (Fig. 2b right side). Qualitative LD increase was also observed by confocal microscope and a 3D reconstruction of both NG and HG samples is exemplified in Fig. 2c.

Glucose effects on fatty acid metabolism

To understand the gene alterations behind the LD modulation, we decided to study the gene expression changes related to the FA metabolism. In HCCs, the most up-regulated genes were HMGCS2 (fold regulation (fr) = 5.42), involved in ketone body metabolism. Increased gene expression was also observed for ACSL6 (fr = 3.74) and ACOT6 (fr = 2.08), embroiled in FA

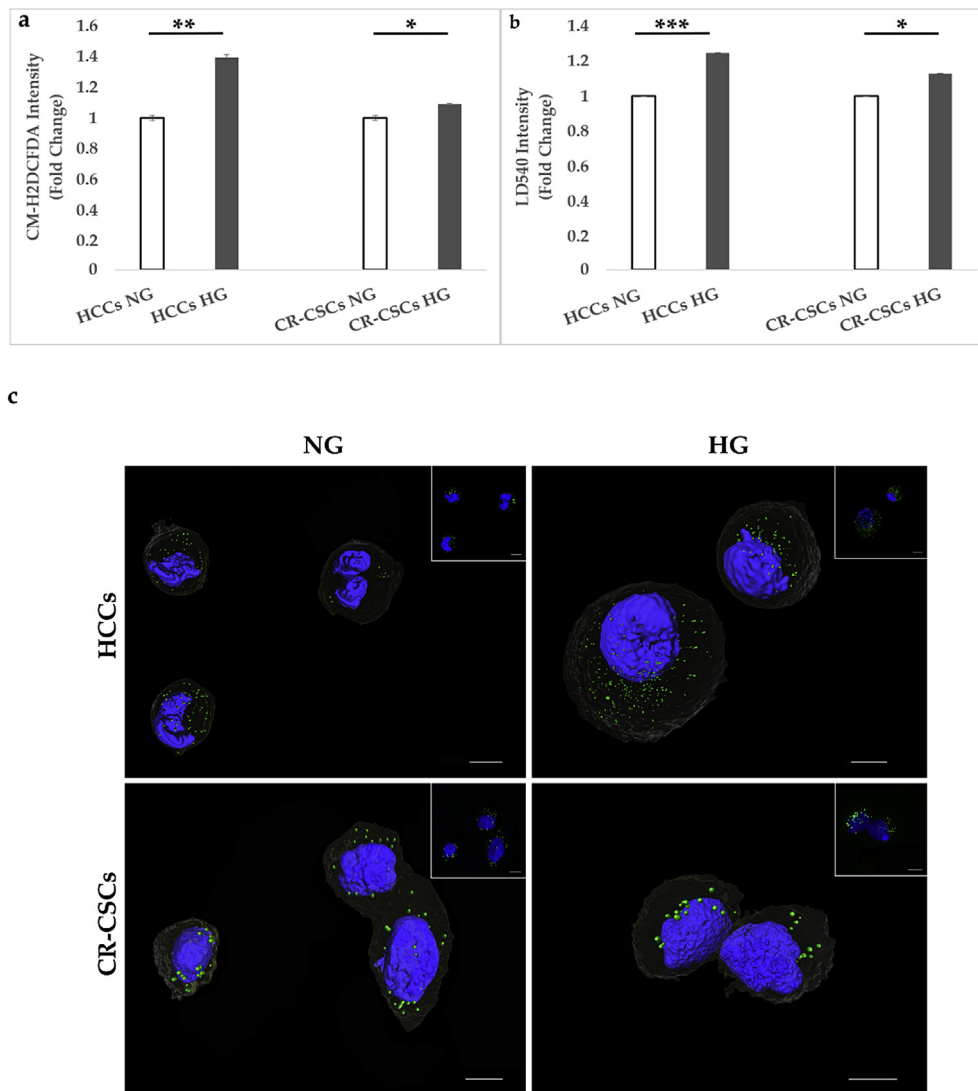


Figure 2 ROS and LD comparison of HG versus NG conditions in both HCCs and CR-CSCs after 72 hrs from the beginning of the treatment. **a)** HCCs and CR-CSCs were collected and stained with CM-H2DCFDA, as reported in the Material and Methods section and analyzed by FACS. A higher increase in ROS was observed in HCCs compared to CR-CSCs. **b)** HCCs and CR-CSCs stained with LD540 were analyzed by FACS. Both samples showed a LD increase in HG, with HCCs being more affected. **c)** 3D reconstruction of both HCCs and CR-CSCs in NG and HG conditions stained with LD540 (green) for visualizing LDs and counterstained with NucBlue (blue) for imaging nuclei. In the inset Max Intensity Projection of the relative z-stack images used for the 3D reconstruction. All images were taken at the confocal microscopes, as reported in Materials and Methods (Section [ROS and LD Quantification](#)) and were mounted with Avizo 9.3. Scale bar is 10 μ m. Note: * $p \leq 0.05$; ** $p \leq 0.01$; *** $p \leq 0.001$.

metabolism, GPD1 (fr = 3.25), encoding for NAD-dependent glycerol-3-phosphate dehydrogenase 1, and FABP4 (fr = 2.13), involved in FA transport. On the other hand, DECR2 (fr = -3.33), an auxiliary peroxisomal enzyme involved in unsaturated FA-oxidation, was down-regulated. In CR-CSCs, PRKAG3, one of the two regulatory subunits of the AMPK, was up-regulated (fr = 3.44) and it was the only gene showing modulation after 72 hrs of HG treatment. [Figs. 3–6](#).

Thus, HG seemed to have a bigger influence on FA metabolism of HCCs than of CR-CSCs, as in the latter almost all the genes analyzed did not exhibit high changes in expression, as compared to NG.

Glucose effects on lipoprotein signaling and cholesterol metabolism

To assess changes in genes involved in the major lipoprotein signaling and cholesterol pathways in response to 72 hrs of HG treatment, PCR Arrays were performed.

In HCCs, 50 mM glucose induced a strong up-regulation of CELA3B (fr = 22.7) and at less extent of APOL1 (fr = 2.11) and CYP11A1 (fr = 2.03), all involved in cholesterol metabolism. Also, CYP7A1, a gene participating in cholesterol catabolism, resulted up-regulated (fr = 6.4). On the other hand, APOL5 (fr = -3.94) and NROB2

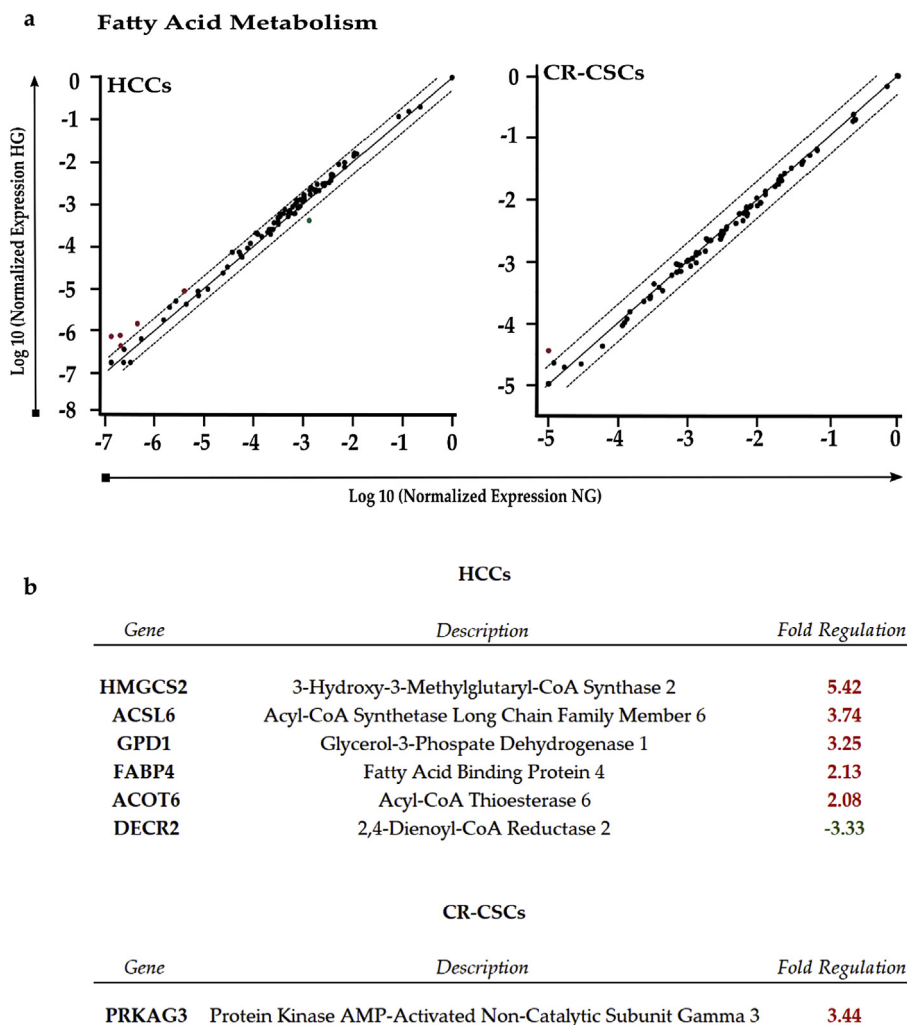


Figure 3 RT2 Profiler PCR analysis of Human Fatty Acid Metabolism. a) Scatter plot of the 84 genes present in the array. Red dots indicate up-regulated genes, while the green dot indicates the down-regulated gene, all compared to NG condition. The central line shows genes that were unchanged with boundaries representing the two-fold regulation cut-off. b) Table reporting all genes affected by the HG concentration in both HCCs and CR-CSCs with the respective fold regulations. Only fold regulations ≥ 2 and p-values ≤ 0.05 were considered.

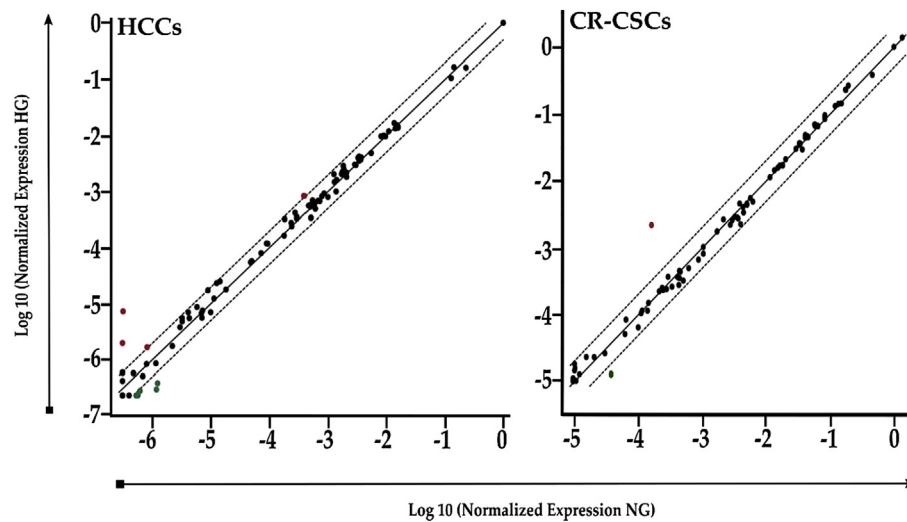
($fr = -3.25$), the former encoding for an intracellular protein likely related with lipid movement and interaction with organelles, the latter encoding for a nuclear repressor (SHP) likely inhibiting steroid hormone pathway, were the most down-regulated genes in HCCs. Negative fold regulation was also observed for PCSK9 ($fr = -2.42$), involved in cholesterol homeostasis being able to control the activity of low-density lipoprotein (LDL) receptors, and AKR1D1 ($fr = -2.3$), which participates in cholesterol catabolism, and STAB2 ($fr = -2.21$), which encodes for a trans-membrane receptor able to bind to LDLs. In CR-CSCs instead, there was only one gene up-regulated, with a highly positive fold regulation ($fr = 13.91$), that was APOA1, whose product is a high-density lipoprotein (HDL)-associated protein with antioxidant activity, participating in cholesterol homeostasis. Furthermore, a decrease in expression was observed for CELA3A ($fr = -2.73$), a gene encoding for an elastase with a potential function in

cholesterol metabolism. In summary, glucose treatment affected the expression of a higher number of lipoprotein signaling- and cholesterol metabolism-related genes in HCCs than in CR-CSCs.

Glucose effects on oxidative stress

ROS gene modulation was also investigated with the same approach pursued for LDs. In HCCs, after glucose treatment, up-regulation was observed for TPO ($fr = 4.79$) gene encoding for protein with antioxidant activity, as well as for NOS2 ($fc = 3.25$), NOX5 ($fc = 3.13$), ALOX12 ($fr = 2.66$), mainly involved in ROS metabolism. Instead in CR-CSCs, decreased expression was reported for NCF1 ($fr = -4.36$). Hence, HG exposure induced only up-regulations of oxidative stress-responsive genes in HCCs, and in CR-CSCs only down-regulation of a gene involved in superoxide anion production.

a Lipoprotein Signaling and Cholesterol Metabolism



b HCCs

<i>Gene</i>	<i>Description</i>	<i>Fold Regulation</i>
CELA3B	Chymotrypsin-like elastase family, member 3A	22.7
CYP7A1	Cytochrome P450, family 7, subfamily A, polypeptide 1	6.4
APOL1	Apolipoprotein L, 1	2.11
CYP11A1	Cytochrome P450, family 11, subfamily A, polypeptide 1	2.03
STAB2	Stabilin 2	-2.21
AKR1D1	Aldo-keto reductase family 1, member D1	-2.3
PCSK9	Proprotein convertase subtilisin/kexin type 9	-2.42
NR0B2	Nuclear receptor subfamily 0, group B, member 2	-3.25
APOL5	Apolipoprotein L, 5	-3.94

CR-CSCs

<i>Gene</i>	<i>Description</i>	<i>Fold Regulation</i>
APOA1	Apolipoprotein A-I	13.91
CELA3A	Chymotrypsin-like elastase family, member 3A	-2.73

Figure 4 RT2 Profiler PCR analysis of Human Lipoprotein Signaling and Cholesterol Metabolism. **a)** Scatter plot of the 84 genes present in the array. Red dots indicate up-regulated genes, while the green ones indicate the down-regulated genes. The central line shows genes that were unchanged with boundaries representing the two-fold regulation cut-off. **b)** Table reporting all genes affected by the HG concentration in both HCCs and CR-CSCs, as compared to NG conditions. Fold regulations ≥ 2 and p-values ≤ 0.05 were considered.

Glucose effects on oncogenes and tumor suppressor genes

When analyzed the expression of oncogenes and tumor suppressors, HCCs showed only down-regulations, such as for BCL2 (fr = -2.23) and MYB (fr = -4.45), considered oncogenes, and RUX3 (fr = -3.3), which is a tumor suppressor gene. Instead, in CR-CSCs, HG treatment did not elicit changes in the genes analyzed by the PCR Array, suggesting that in cancerous cells HG did not strongly affect

the expression of genes whose behavior could be already altered.

Dysregulation of lipid metabolism and oxidative stress pathways drives CRC progression

Despite the fact that the prognostic impact of high blood sugar levels on CRC initiation and progression has been an unexplored topic for a long time, recent studies have demonstrated that hyperglycemia is involved in several

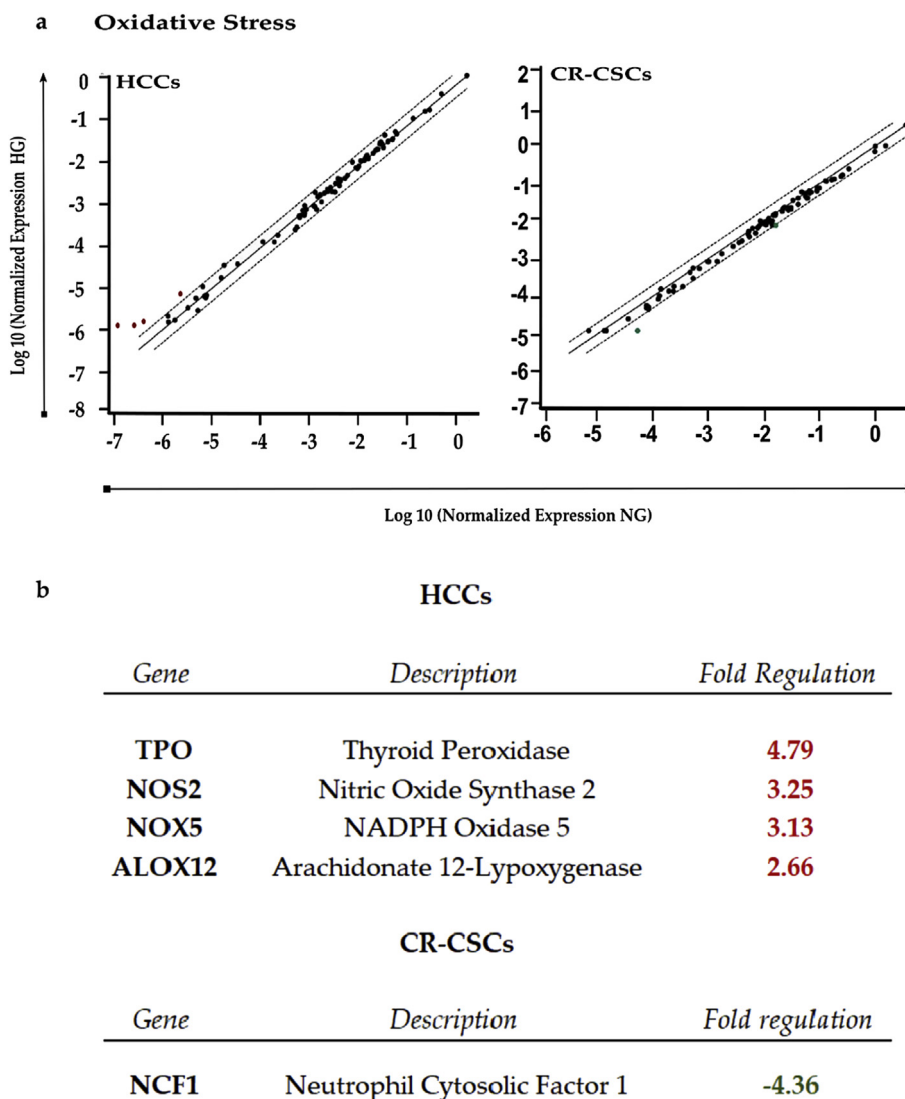


Figure 5 RT2 Profiler PCR analysis of Human Oxidative Stress. a) Scatter plot of the 84 genes present in the array. Red dots indicate up-regulated genes, while the green one indicates the only down-regulated gene. The central line shows genes that were unchanged with boundaries representing the two-fold regulation cut-off. b) Table reporting all genes affected by the HG concentration in both HCCs and CR-CSCs, as compared to NG conditions. Only fold regulations ≥ 2 and a p-values ≤ 0.05 were considered.

mechanisms promoting both tumor initiation³¹ and progression,³² with the regulation of crucial phenomena underlying CRC patients survival. On this regard, the acquisition of a mesenchymal/invasive phenotype³³ and the acquired chemoresistance are fundamental for CRC patients prognosis.³⁴ Given that CSCs are considered to drive all the above-mentioned steps of tumorigenesis, we decided to investigate the clinical impact of the differentially expressed genes of CR-CSCs upon treatment with HG. Importantly, our data indicate that higher expression levels of PRKAG3 and APOA1 which were upregulated upon HG cell culture conditions, significantly correlate with a worse prognosis for CRC patients, as indicated by the Kaplan Meier showing the relapse free survival (RFS) probability (Fig. 7). Differently, high expression levels of CELA3A and NCF1, that were downregulated following HG treatment, show a significant association with better survival rates (Fig. 7).

Drug treatments

Since an increase of the LD amount was observed in both cell lines grown in glucose enriched media, HCC and CR-CSC mortality was analyzed upon treatment with two drugs interfering with lipid metabolism, namely Atorvastatin (10 μM) and PF-06424439 (10 μM). In particular, Atorvastatin works inhibiting the 3-hydroxymethyl-3-glutaryl (HMG)-coenzyme A (CoA) reductase (HMGCR) to competitively block the conversion of HMG-CoA to mevalonate, which is a precursor in the synthesis of cholesterol.³⁵ It is usually used to treat dyslipidemia that can also occur in type 2 diabetes mellitus. Instead, PF-06424439 is an inhibitor of the diacylglycerol acyltransferase 2 (DGAT2) enzyme, which catalyzes the final step in the synthesis of TAGs, thus likely impairing FA synthesis and LD formation.³⁶ Cell mortality was also analyzed after 10 μM of Oxaliplatin treatment,

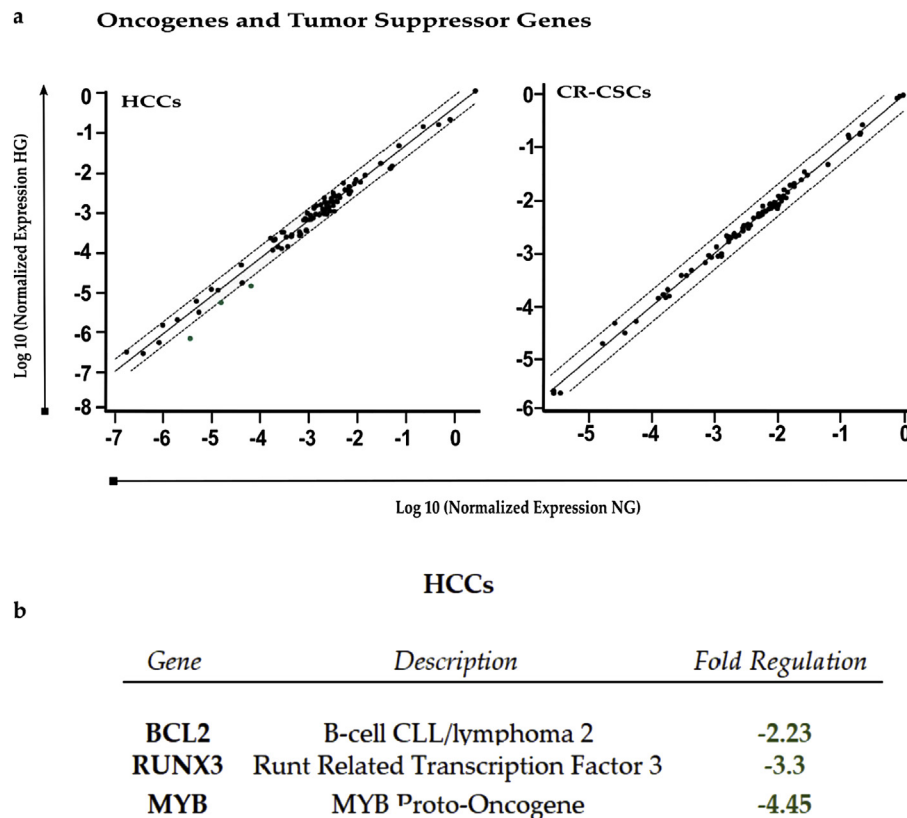


Figure 6 RT2 Profiler PCR analysis of Human Oncogenes and Tumor Suppressor Genes. a) Scatter plot of the 84 genes present in the array. Green dots indicate down-regulated genes. The central line indicates genes that were unchanged with boundaries representing the two-fold regulation cut-off. b) Table reporting all genes affected by the HG concentration in both HCCs and CR-CSCs, as compared to NG. Only fold regulations ≥ 2 and p-values ≤ 0.05 were considered.

chosen because it is a platinum-based chemotherapy agent commonly used for treating CRC.³⁷ Results from flow cytometry analysis of dead cells after 24, 48 and 72 hrs of drug treatments in NG are shown in Fig. 8. While in HCCs all the tested drugs did not induce significant mortality overtime (Fig. 8a), in CR-CSCs at 48 and 72 hrs both Oxaliplatin (91% and 171%, respectively) and Atorvastatin (78% and 488%, respectively) increased cell mortality compared to the untreated cells (Fig. 8b). By contrast, PF-06424439 did not seem to have effects on cell death at each time point, as compared to the controls (Fig. 8b).

To evaluate whether additional effects could be obtained by combined use of drugs, CR-CSC mortality was studied in NG media in a time course experiment (Fig. 8c). All the double combinations resulted in a significant time-dependent increase in cell mortality. Particularly, while at 24 hrs the combined treatments did not result in strong differences in cell death (30% for Oxaliplatin/PF-06424439; 58% for Oxaliplatin/Atorvastatin; 43% for Atorvastatin/PF-06424439) compared to the control, at 48 hrs and much more at 72 hrs huge effects were observed with Oxaliplatin/Atorvastatin (128% at 48 hrs and 517% at 72 hrs) and Atorvastatin/PF-06424439 (230% at 48 hrs and 1000% at 72 hrs).

Thus, higher effects were exhibited by the combination of Atorvastatin with PF-06424439 in the long run. Moreover, under conditions of excessive glucose availability, the highest impact on CR-CSC mortality was exerted by

Atorvastatin, indicating that statin in combination with HG could sensitize CR-CSCs to death especially after 72 hrs (Fig. 8d).

Discussion

LDs are nowadays well recognized as important players in CRC development and stemness,^{24,38} and they have been proposed as a new functional marker in CR-CSCs.²⁴ Moreover, the desaturation level of lipids present inside LDs was also suggested as a metabolic stem cell marker in ovarian cancer.³⁹

Recent shreds of evidence highlighted a possible role of metabolic alterations in inducing malignant transformation, and in this context, glucose and lipid metabolisms and their interplay are currently areas of expanding interests. It is still unclear to which extent a glucose excess could affect cancer cells, in particular CSC stemness and trigger the LD accumulation. Besides, few reports have in-depth documented the effects of HG concentrations in non-malignant colon cells.

Based on these considerations, in the present experimental work, we studied the effects of 72 hrs exposure to HG concentrations in healthy and in cancer stem cells. The goal was to investigate the effects of an excess of glucose that represents an extreme circumstance of pathological conditions. Firstly, we found that in CR-CSCs HG elicited

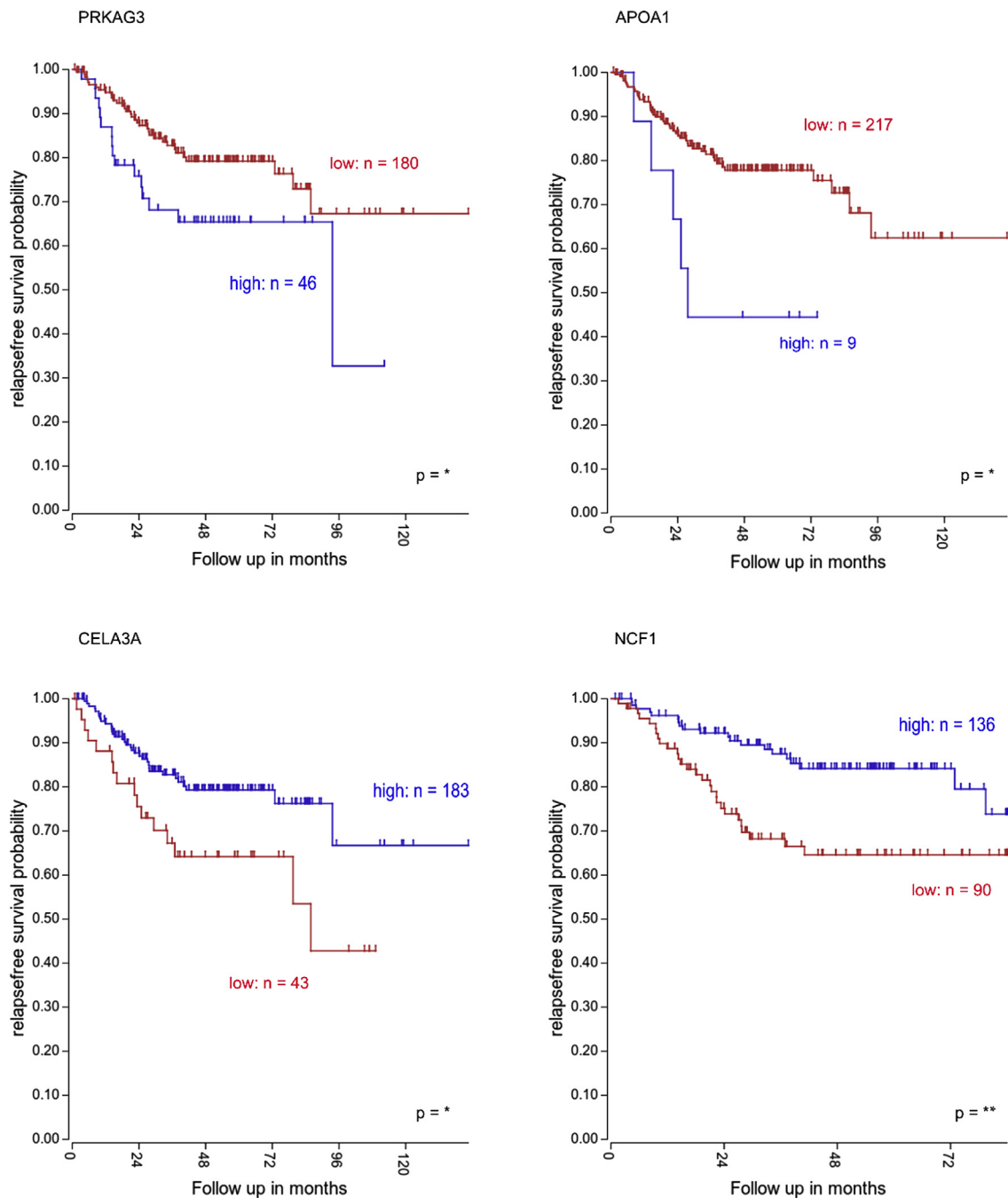


Figure 7 Clinical impact of genes involved in lipid metabolism and oxidative stress. Relapse-free survival (RFS) rate of CRC patients (Tumor Colon-Sieber database) according to PRKAG3, APOA1, CELA3A and NCF1 expression levels.

activation of the PI3K/AKT pathway and a higher expression of stemness markers (CD133 and CD44v6), associated with a reduced growth (data not shown), thus pointing out the importance of glucose as a crucial nutrient for CR-CSCs. Also, this evidence suggested that glucose concentration in the tumor microenvironment might significantly affect CSC behavior and aggressiveness.

Secondly, a significant induction of ROS was observed upon HG treatment in both cell lines. This observation was in agreement with other studies showing an increase of ROS in hyperglycemic conditions, presumably resulting from an

overburdened mitochondrial electron transport chain or hyperactivated enzymatic systems, including NOX and NOS enzymes.^{40,41} Moreover, high ROS were also accompanied by a simultaneous overproduction of LDs both in healthy and CR-CSCs, which suggested that the excess of glucose might be, at least in part, converted and stored as lipids (cholesterol and triglycerides) in the form of LDs, as already reported in literature.^{42,43} In healthy and cancer cells, LDs might have a protective role against lipotoxicity, as well as be an essential source of energy.⁴⁴ However, the observed ROS and LD over-loading following long-term glucose

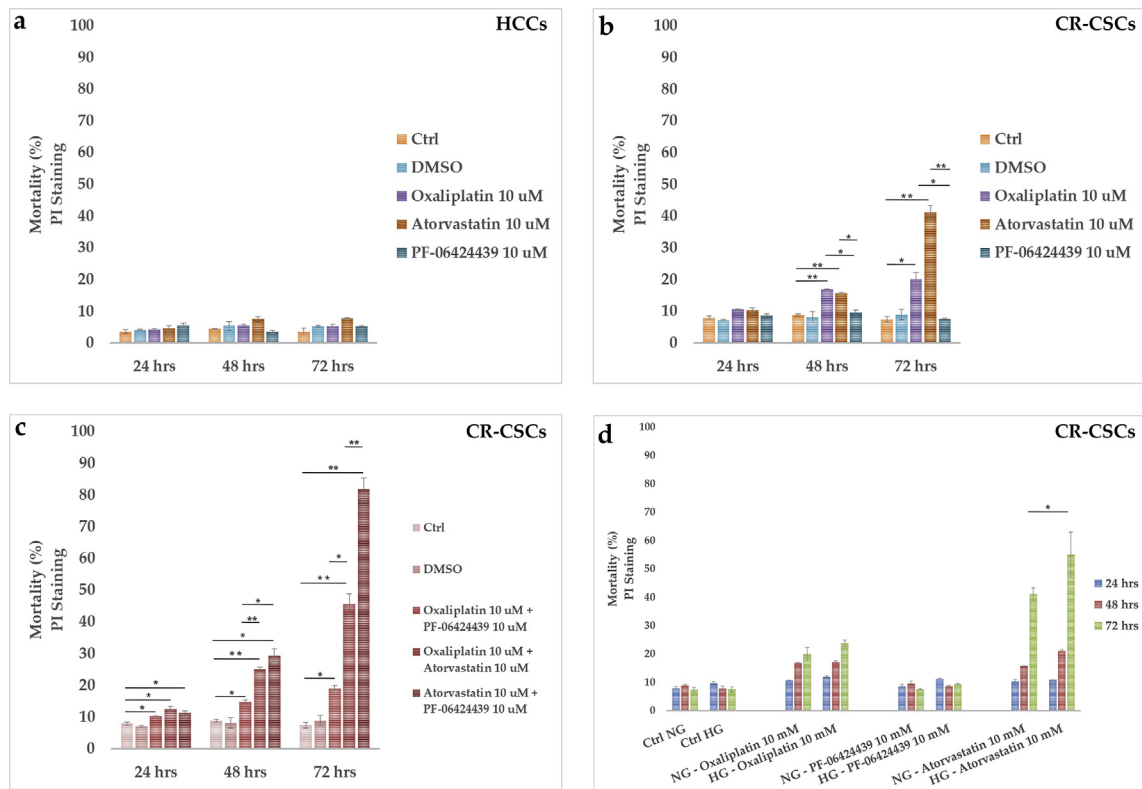


Figure 8 Cell death analysis and comparison between Oxaliplatin, Atorvastatin and PF-06424439 in HCCs and CR-CSCs. a) HCCs have been treated with Oxaliplatin 10 μ M, Atorvastatin 10 μ M or PF-06424439 10 μ M for 72 hrs. Afterwards, cells were collected, stained with PI and analyzed by FACS. b) CR-CSCs were treated as HCCs and stained with PI. c) The drugs were used in double combinations in order to obtain a possible synergistic effect in killing CR-CSCs; d) single drug treatments (Oxaliplatin, PF-06424439 and Atorvastatin, 10 μ M all) were tested on CR-CSCs both in NG and HG. Note: * $p \leq 0.05$; ** $p \leq 0.01$; *** $p \leq 0.001$.

supplementation might also impair cellular functions. In fact, it has been well documented that high ROS levels promoted inflammation and that their increase, following excessive glucose intake, induced LD accumulation and could lead to pathophysiological conditions, including diabetes, obesity, aging and cancer.^{45–47} It has also been reported that increased ROS formation resulted in peroxidized LD accumulation in glia and the two conditions together could cause neurodegeneration.⁴⁸ Thereby, regulation of genes involved in oxidative stress, FA and cholesterol metabolism was also evaluated after prolonged HG exposure. Our qPCR array data revealed that, in response to increased availability of glucose, HCCs mainly up-regulated oxidative stress-responsive genes and superoxide metabolism genes. Notably, NOS2, NOX5 and ALOX2 genes resulted increased, the former of which encodes for an enzyme responsible for the production of nitric oxide (NO), which, in addition to be a signaling molecule, is also involved in inflammatory responses and, by interaction with superoxide anion ($O_2^{\cdot-}$) can cause oxidative damages.⁴⁹ In fact, NOS2 overproduction can inhibit the mitochondrial electron transport chain, induce DNA strand breaks and has been associated with poor cancer prognosis.^{49,50} NOX5 encodes for a NADPH oxidase that generates $O_2^{\cdot-}$ and, like for NOS2, its increased expression has been reported in different type of cancers.⁵¹ Instead, ALOX 12 protein is a lipoxygenase, which catalyzes the peroxidation of

polyunsaturated FA, thus producing bioactive lipids and ROS, which in turn can stimulate inflammation and promote oxidative stress.⁵² Interestingly, elevated expression of this gene has been observed in pancreatic and brain cells in response to hyperglycemia.^{53–55} Surprisingly, our data highlighted a particular and unexpected Thyroid peroxidase (TPO) overexpression in HG-treated HCCs. In fact, TPO is typically expressed in the thyroid gland, however a recent work has shown its expression also in the healthy and cancerous breast tissues,⁵⁶ while activated thyroid hormones were increased in CR-CSCs in which induced differentiation and sensitization of CR-CSCs.⁵⁷ To date, we do not know the role of TPO in the healthy colon cells under high glucose conditions, but its ability to use hydrogen peroxide might be involved. Further investigations to establish TPO role and function in presence of excess of glucose are needed and remain to be elucidated.

In our study, the over-activation of such oxidative stress-related genes suggested for a potential effect of HG exposure in promoting an inflammatory status in HCCs. As far as the lipid metabolism is concerned, in HCCs we found overexpression of genes encoding for enzymes in cholesterol, FA and TAG metabolisms and lipid trafficking. On the other hand, HCCs in the same culture conditions down-regulated genes encoding mainly for a LDL receptor, LDL- or HDL-associated proteins, as well as an enzyme in cholesterol catabolism and an enzyme involved in FA β -oxidation.

These observations pointed out to modulation of intracellular lipid accumulation and a reduction of circulating cholesterol uptake. Of interest, FABP4, one of the up-regulated genes in HCCs, has been proposed to be involved in lipid transport to LDs for their storage that is in line with our evidence of LD increased expression, as well as to peroxisomes for oxidation.^{58,59} Studies also showed that its up-regulation was correlated with the development of inflammation, insulin resistance, diabetes mellitus and obesity.^{58,60,61} Importantly, a recent work from Hao and collaborators showed that elevated levels of circulating FABP-4 were present in obese women with breast cancer. In the same study, treatments with FABP-4 induced stemness and aggressiveness of mammary cancer cells both *in vitro* and *in vivo*, as well as tumor development, through IL-6/STAT3/ALDH1 pathway, thus revealing a new link between obesity and breast cancer.⁶² In light of these results, understanding if and how enhanced FABP-4 expression and LD increase in hyperglycemic conditions might be linked and involved in CR tumor development deserves further investigations.

Interestingly, in HCCs a strong up-regulation was observed for HMGCS2 gene, encoding for a rate-limiting enzyme involved in the synthesis of ketone bodies, mostly produced during starvation from the breakdown of FAs. This finding suggested that HCCs might be capable of metabolizing ketone bodies. In recent studies, it has been shown that ketone bodies can support cancer growth in environments where the nutrient supply is limiting^{63,64} and HMGCS2 has also been proposed as an apocrine cancer biomarker.^{65,66} Here instead, we found its marked upregulation in a HG enriched medium, where energy availability should be not limiting. HMGCS2 is a mitochondrial enzyme, so it may be possible that oxidative stress induced by HG impairs mitochondrial functions that could account for this observation. Taken together, these findings raise the possibility that very HG conditions might produce an excess of FAs that, in turn, may be directed towards the storage, but also to their activation and ketogenesis, despite HG availability. To date, the reasons for these responses remain to be clarified, but they could be the expression of dysregulated metabolic pathways activated/inhibited in HG conditions. HCCs grown in HG for 72 hrs also showed decreased expression of pro-apoptotic and tumor suppressor genes. As an example, the oncosuppressor gene RUNX3 was down-regulated in HG-treated HCCs. Reduced levels of its expression have been associated with poor prognosis in patients with CRC,⁶⁷ and Runx3-null gastric cells showed epithelial–mesenchymal transition and tumorigenic stem cell-like features.⁶⁸ To our knowledge, here we reported for the first time a relationship between hyperglycemia and RUNX3-reduced mRNA levels that may provide a potential link with tumorigenesis.

Conversely, in CR-CSCs, 72 hrs of HG treatment did not seem to induce massive gene regulations. We noticed the down-regulation of NCF1, the regulatory cytosolic subunit of phagocytic NADPH oxidase complex. NCF1 in fact activates the complex, which subsequently produces O₂–•, an essential mechanism in immune system. Glucose excess seemed to affect the regulatory mechanisms of the complex that might induce lower superoxide production, even though further studies are required, as currently NCF1 role

in non-phagocytic cells is poorly investigated and unexplored in CSCs.

Up-regulation was also found for PRKAG3 gene, which encodes for an AMPK regulatory subunit which activates the AMPK enzyme. Instead, the AMPK catalytic subunit gene was not affected by HG exposure (data not shown). AMPK is considered an energy sensor in the crosstalk between multiple metabolic pathways and, when active, negatively regulates the PI3K/AKT signaling cascade.⁶⁹ Over activation of the PI3K/AKT pathway, which promotes survival and proliferation, is frequently associated with different types of tumors, including CRC.^{27,70} Moreover, it has been documented that AKT signaling stimulates glucose uptake and ATP production, indirectly hindering AMPK activation.⁷¹ In the present study, we showed higher expression of PI3K and AKT proteins in CR-CSCs under HG conditions, thus allowing us to speculate that increased signaling activity of PI3K/AKT pathway could inhibit AMPK and this could in somehow correlate with the higher PRKAG3 mRNA levels observed in HG. It is also noteworthy that AMPK inactivation stimulates lipid synthesis⁷² suggesting a potential connection between activated PI3/AKT cascade and LD accumulation seen after long term HG exposure.^{73,74} Indeed, Vereshchagina *et al.* showed that elevated activation of AKT in *Drosophila* nurse cells induced to enlarged LDs and high expression of the fly homologue perilipin.⁷⁵

In our hyperglycemic conditions, APOA1 gene, responsible for the expression of the main HDL-associated protein which also participates in cholesterol efflux and reverse transport, resulted strongly upregulated in CR-CSCs. It has been recently showed that increased levels of APOA1/HDL might protect against the onset of CRC,⁷⁶ although the mechanisms remain unfathomed. We also observed a substantial decrease in CELA3A mRNA in CR-CSCs. This gene encodes for an elastase usually produced by pancreas with digestive function and potentially able to bind cholesterol even though its functional role in CRC remains to be elucidated. However, better survival rates in patients were associated with higher and lower expression levels of APOA1 and CELA3A genes, respectively. Altogether these observations raise the intriguing possibility that cholesterol, whose esterified form is a component of LDs, might play a crucial role in CR-CSC biology. A recent work from Wang and colleagues highlighted a potential link between an excess of cholesterol and increased growth of colonic stem cells and, consequently, accelerated CRC development.⁷⁷ Thereby, the evidence of LD increase in CR-CSCs in response to HG might be involved in processes linked to CR-CSC survival in metabolic stress conditions. Thus, in the present work, we tested the effects of Atorvastatin, a commonly used statin inhibiting HMG-CoA reductase, on cell viability when interfering with the cholesterol synthesis pathway, and compared with PF-06424439, an inhibitor of diacylglycerol acyltransferase (DGAT2) involved in the synthesis of TAGs, and Oxaliplatin, a commonly used chemotherapy drug for CRC.

In the last few years, both Atorvastatin and PF-06424439 have been largely studied as potential anti-cancer drugs, and the molecular mechanisms involved in the lipid pathway inhibition are well described elsewhere,⁷⁸ although results from the literature are conflicting. Here, we showed that Atorvastatin induced the highest mortality

on CR-CSCs after 72 hrs in NG, without affecting the healthy counterpart. Noteworthy, when Atorvastatin was used in combination with PF-06424439, a dramatic increase in cell mortality was obtained after 72 hrs. This indicated that by hindering both cholesterol and TAGs synthesis, synergistic effects were markedly induced, as the PF-06424439 alone was not able to kill cells at any time point. Then, when analyzed the effect of Atorvastatin in the presence of HG, CR-CSC mortality was increased compared to NG and, of note, it was the only treatment able to exert this effect in HG. Indeed, a recent paper from Sierra Gonzales and co-workers has showed that supplementation with 25 mM mannose, a derivative of glucose, reduced cancer cell growth and, in combination with chemotherapy drugs, made cells more sensitive to death *in vitro* and *in vivo*.⁷⁹ Here we showed enhanced cell death in presence of 50 mM glucose and 10 μ M Atorvastatin on the cancer stem population. These preliminary findings suggested that statins may better interfere with CR-CSC growth in an enriched glucose availability. Given the high FA and cholesterol requirements of cancer cells for proliferation together with the oxidative stress induced in response to HG concentrations, the well documented dual (lipid-lowering and antioxidant) effect of Atorvastatin⁸⁰ could explain these observations.

Conclusions

In conclusion, we demonstrated that 72 hrs of HG supplementation was sufficient to increase ROS and to accumulate LDs in both HCCs and CR-CSCs. In the latter population, HG was also responsible for the increase of the stemness markers and AKT activation, highlighting a tight correlation between high tumorigenicity and LD generation. Moreover, in our culture conditions, HG modulated transcription of many genes related to FA metabolism, apolipoproteins signaling, cholesterol metabolism, oxidative stress, oncogenes and tumor suppressors, at a greater extent in HCCs than in CR-CSCs.

Although the link between increased ROS and LDs and enhanced risk of CR cancer in response to very HG conditions warrants further investigations and more detailed experiments are required in order to elucidate the underlying mechanistic links, our preliminary data provide useful evidence to study the process involved in tumorigenesis and cancer maintenance.

These results provide novel insights into the role of glucose in metabolic alterations and might help to disclose possible mechanisms for HG role in tumorigenesis. In metabolic stress conditions LDs might work as a potential functional marker not only in CR-CSCs, but also in the healthy counterpart. In addition, our findings might be useful to highlight potential targets of glucose or lipid pathways for the therapeutic treatment of CRC and, in particular, to eradicate CR-CSCs.

Data availability

All data generated or analyzed during this study are included in this published article. Upon request raw data would be made available.

Conflict of Interest

Authors declare no conflict of interest.

Acknowledgments

This study was supported by Italian Association for Cancer Research (AIRC) and from the European Union's Horizon 2020 Research And Innovation Programme under the Marie Skłodowska-Curie grant agreement No 800924. This work was also supported by AIRC (5x1000 Clinical Oncology Extension Program 9979 and IG 16746).

The authors acknowledge financial support from King Abdullah University of Science and Technology for OCRF-2014-CRG and OCRF-2016-CRG grants and from Piedmont Region through European Funds for Regional Development ("Food Digital Monitoring" project).

This work is dedicated to the memory of our beloved Prof. Giovanni Morrone.

Appendix A. Supplementary data

Supplementary data to this article can be found online at <https://doi.org/10.1016/j.gendis.2019.09.010>.

References

1. Brouns F. WHO Guideline: "Sugars intake for adults and children" raises some question marks. *Agro Food Ind Hi Tech*. 2015; 26(4):34–36.
2. Morenga LT, Mallard S, Mann J. Dietary sugars and body weight: systematic review and meta-analyses of randomised controlled trials and cohort studies. *Bmj-Brit Med J*. 2013;346.
3. Yang QH, Zhang ZF, Gregg EW, Flanders D, Merritt R, Hu FB. Added sugar intake and cardiovascular diseases mortality among US adults. *Jama Intern Med*. 2014;174(4):516–524.
4. Brownlee M. Biochemistry and molecular cell biology of diabetic complications. *Nature*. 2001;414(6865):813–820.
5. Cairns RA, Harris IS, Mak TW. Regulation of cancer cell metabolism. *Nat Rev Cancer*. 2011;11(2):85–95.
6. Hay N. Reprogramming glucose metabolism in cancer: can it be exploited for cancer therapy? *Nat Rev Cancer*. 2016;16(10): 635–649.
7. Romieu I, Ferrari P, Rinaldi S, et al. Dietary glycemic index and glycemic load and breast cancer risk in the European prospective investigation into cancer and nutrition (EPIC). *Am J Clin Nutr*. 2012;96(2):345–355.
8. Hanahan D, Weinberg RA. Hallmarks of cancer: the next generation. *Cell*. 2011;144(5):646–674.
9. Baenke F, Peck B, Miess H, Schulze A. Hooked on fat: the role of lipid synthesis in cancer metabolism and tumour development. *Dis Model Mech*. 2013;6(6):1353–1363.
10. Zheng J. Energy metabolism of cancer: glycolysis versus oxidative phosphorylation (Review). *Oncol Lett*. 2012;4(6): 1151–1157.
11. DeBerardinis RJ, Lum JJ, Hatzivassiliou G, Thompson CB. The biology of cancer: metabolic reprogramming fuels cell growth and proliferation. *Cell Metabol*. 2008;7(1):11–20.
12. Cerutti PA. Prooxidant states and tumor promotion. *Science*. 1985;227(4685):375–381.
13. Fiaschi T, Chiarugi P. Oxidative stress, tumor microenvironment, and metabolic reprogramming: a diabolic liaison. *Int J Cell Biol*. 2012;762825.

14. Padanad MS, Konstantinidou G, Venkateswaran N, et al. Fatty acid oxidation mediated by Acyl-CoA synthetase long chain 3 is required for mutant KRAS lung tumorigenesis. *Cell Rep*. 2016;16(6):1614–1628.
15. Currie E, Schulze A, Zechner R, Walther TC, Farese Jr RV. Cellular fatty acid metabolism and cancer. *Cell Metabol*. 2013;18(2):153–161.
16. Farese Jr RV, Walther TC. Lipid droplets finally get a little R-E-S-P-E-C-T. *Cell*. 2009;139(5):855–860.
17. Cotte AK, Aires V, Fredon M, et al. Lysophosphatidylcholine acyltransferase 2-mediated lipid droplet production supports colorectal cancer chemoresistance. *Nat Commun*. 2018;9(1):322.
18. Petan T, Jarc E, Jusovic M. Lipid droplets in cancer: guardians of fat in a stressful World. *Molecules*. 2018;23(8):1941.
19. Accioly MT, Pacheco P, Maya-Monteiro CM, et al. Lipid bodies are reservoirs of cyclooxygenase-2 and sites of prostaglandin-E-2 synthesis in colon cancer cells. *Cancer Res*. 2008;68(6):1732–1740.
20. Bensaad K, Favaro E, Lewis CA, et al. Fatty acid uptake and lipid storage induced by HIF-1 α contribute to cell growth and survival after hypoxia-reoxygenation. *Cell Rep*. 2014;9(1):349–365.
21. de Gonzalo-Calvo D, Lopez-Vilaro L, Nasarre L, et al. Intratumor cholesteryl ester accumulation is associated with human breast cancer proliferation and aggressive potential: a molecular and clinicopathological study. *BMC Cancer*. 2015;15:460.
22. Nieva C, Marro M, Santana-Codina N, Rao S, Petrov D, Sierra A. The lipid phenotype of breast cancer cells characterized by Raman microspectroscopy: towards a stratification of malignancy. *PLoS One*. 2012;7(10):e46456.
23. Di Franco S, Mancuso P, Benfante A, et al. Colon cancer stem cells: bench-to-bedside-new therapeutical approaches in clinical oncology for disease breakdown. *Cancers (Basel)*. 2011;3(2):1957–1974.
24. Tirinato L, Liberale C, Di Franco S, et al. Lipid droplets: a new player in colorectal cancer stem cells unveiled by spectroscopic imaging. *Stem Cells*. 2015;33(1):35–44.
25. Engelman JA. Targeting PI3K signalling in cancer: opportunities, challenges and limitations. *Nat Rev Cancer*. 2009;9(8):550–562.
26. Vermeulen L, Todaro M, Mello FD, et al. Single-cell cloning of colon cancer stem cells reveals a multi-lineage differentiation capacity. *Proc Natl Acad Sci USA*. 2008;105(36):13427–13432.
27. Todaro M, Gaggiani M, Catalano V, et al. CD44v6 is a marker of constitutive and reprogrammed cancer stem cells driving colon cancer metastasis. *Cell Stem Cell*. 2014;14(3):342–356.
28. Todaro M, Alea MP, Di Stefano AB, et al. Colon cancer stem cells dictate tumor growth and resist cell death by production of interleukin-4. *Cell Stem Cell*. 2007;1(4):389–402.
29. Kemper K, Sprick MR, de Bree M, et al. The AC133 epitope, but not the CD133 protein, is lost upon cancer stem cell differentiation. *Cancer Res*. 2010;70(2):719–729.
30. Fruman DA, Rommel C. PI3K and cancer: lessons, challenges and opportunities. *Nat Rev Drug Discov*. 2014;13(2):140–156.
31. Vulcan A, Manjer J, Ohlsson B. High blood glucose levels are associated with higher risk of colon cancer in men: a cohort study. *BMC Cancer*. 2017;17(1):842.
32. Vasconcelos-dos-Santos A, Loponte HFBR, Mantuano NR, et al. Hyperglycemia exacerbates colon cancer malignancy through hexosamine biosynthetic pathway. *Oncogenesis*. 2017;6(3):e306.
33. Wu JY, Chen JY, Xi Y, et al. High glucose induces epithelial-mesenchymal transition and results in the migration and invasion of colorectal cancer cells. *Exp Ther Med*. 2018;16(1):222–230.
34. Ikemura M, Hashida T. Effect of hyperglycemia on antitumor activity and survival in tumor-bearing mice receiving Oxaliplatin and fluorouracil. *Anticancer Res*. 2017;37(10):5463–5468.
35. Liao JK, Laufs U. Pleiotropic effects of statins. *Annu Rev Pharmacol*. 2005;45:89–118.
36. Kuo A, Lee MY, Sessa WC. Lipid droplet biogenesis and function in the endothelium. *Circ Res*. 2017;120(8):1289–1297.
37. Alcindor T, Beauger N. Oxaliplatin: a review in the era of molecularly targeted therapy. *Curr Oncol*. 2011;18(1):18–25.
38. Tirinato L, Pagliari F, Limongi T, et al. An overview of lipid droplets in cancer and cancer stem cells. *Stem Cell Int*. 2017;1656053.
39. Li J, Condello S, Thomes-Pepin J, et al. Lipid desaturation is a metabolic marker and therapeutic target of ovarian cancer stem cells. *Cell Stem Cell*. 2017;20(3):303–314.
40. Yu TZ, Robotham JL, Yoon Y. Increased production of reactive oxygen species in hyperglycemic conditions requires dynamic change of mitochondrial morphology. *P Natl Acad Sci USA*. 2006;103(8):2653–2658.
41. Turrens JF. Mitochondrial formation of reactive oxygen species. *J Physiol-London*. 2003;552(2):335–344.
42. Li JJ, Cheng JX. Direct visualization of de novo lipogenesis in single living cells. *Sci Rep-Uk*. 2014;4:6807.
43. Guillet-Deniau I, Pichard AL, Kone A, et al. Glucose induces de novo lipogenesis in rat muscle satellite cells through a sterol-regulatory-element-binding-protein-1c-dependent pathway. *J Cell Sci*. 2004;117(10):1937–1944.
44. Bozza PT, Viola JP. Lipid droplets in inflammation and cancer. *Prostaglandins Leukot Essent Fatty Acids*. 2010;82(4–6):243–250.
45. Jin Y, Tan YJ, Chen LP, Liu Y, Ren ZQ. Reactive oxygen species induces lipid droplet accumulation in HepG2 cells by increasing perilipin 2 expression. *Int J Mol Sci*. 2018;19(11):3445.
46. Hotamisligil GS. Inflammation and metabolic disorders. *Nature*. 2006;444(7121):860–867.
47. Panahi G, Pasalar P, Zare M, Rizzuto R, Meshkani R. High glucose induces inflammatory responses in HepG2 cells via the oxidative stress-mediated activation of NF-kappa B, and MAPK pathways in HepG2 cells. *Arch Physiol Biochem*. 2018;124(5):468–474.
48. Liu L, Zhang K, Sandoval H, et al. Glial lipid droplets and ROS induced by mitochondrial defects promote neurodegeneration. *Cell*. 2015;160(1–2):177–190.
49. Forstermann U, Sessa WC. Nitric oxide synthases: regulation and function. *Eur Heart J*. 2012;33(7):829.
50. Thomas DD, Wink DA. NOS2 as an emergent player in progression of cancer. *Antioxidants Redox Signal*. 2017;26(17):963–965.
51. Brar SS, Corbin Z, Kennedy TP, et al. NOX5 NAD(P)H oxidase regulates growth and apoptosis in DU 145 prostate cancer cells. *Am J Physiol Cell Physiol*. 2003;285(2):C353–C369.
52. Chen M, Yang ZD, Smith KM, Carter JD, Nadler JL. Activation of 12-lipoxygenase in proinflammatory cytokine-mediated beta cell toxicity. *Diabetologia*. 2005;48(3):486–495.
53. Laybutt DR, Sharma A, Sgroi DC, Gaudet J, Bonner-Weir S, Weir GC. Genetic regulation of metabolic pathways in beta-cells disrupted by hyperglycemia. *J Biol Chem*. 2002;277(13):10912–10921.
54. Taha AY, Gao F, Ramadan E, Cheon Y, Rapoport SI, Kim HW. Upregulated expression of brain enzymatic markers of arachidonic and docosahexaenoic acid metabolism in a rat model of the metabolic syndrome. *BMC Neurosci*. 2012;13:131.
55. Tersey SA, Bolanis E, Holman TR, Maloney DJ, Nadler JL, Mirmira RG. 12-Lipoxygenase and islet beta-cell dysfunction in diabetes. *Mol Endocrinol*. 2015;29(6):791–800.

56. Godlewska M, Arczewska KD, Rudzinska M, et al. Thyroid peroxidase (TPO) expressed in thyroid and breast tissues shows similar antigenic properties. *PLoS One*. 2017;12(6):e0179066.
57. Catalano V, Dentice M, Ambrosio R, et al. Activated thyroid hormone promotes differentiation and chemotherapeutic sensitization of colorectal cancer stem cells by regulating Wnt and BMP4 signaling. *Cancer Res*. 2016;76(5):1237–1244.
58. Makowski L, Brittingham KC, Reynolds JM, Suttles J, Hotamisligil GS. The fatty acid-binding protein, aP2, coordinates macrophage cholesterol trafficking and inflammatory activity. Macrophage expression of aP2 impacts peroxisome proliferator-activated receptor gamma and IkappaB kinase activities. *J Biol Chem*. 2005;280(13):12888–12895.
59. Hotamisligil GS, Bernlohr DA. Metabolic functions of FABPs—mechanisms and therapeutic implications. *Nat Rev Endocrinol*. 2015;11(10):592–605.
60. Uysal KT, Scheja L, Wiesbrock SM, Bonner-Weir S, Hotamisligil GS. Improved glucose and lipid metabolism in genetically obese mice lacking aP2. *Endocrinology*. 2000;141(9):3388–3396.
61. Furuhashi M, Hotamisligil GS. Fatty acid-binding proteins: role in metabolic diseases and potential as drug targets. *Nat Rev Drug Discov*. 2008;7(6):489–503.
62. Hao JQ, Zhang YW, Yan XF, et al. Circulating adipose fatty acid binding protein is a new link underlying obesity-associated breast/mammary tumor development. *Cell Metabol*. 2018;28(5):689.
63. Dueregger A, Schopf B, Eder T, et al. Differential utilization of dietary fatty acids in benign and malignant cells of the prostate. *PLoS One*. 2015;10(8).
64. Martinez-Outschoorn UE, Lin Z, Whitaker-Menezes D, Howell A, Sotgia F, Lisanti MP. Ketone body utilization drives tumor growth and metastasis. *Cell Cycle*. 2012;11(21):3964–3971.
65. Bonuccelli G, Tsigos A, Whitaker-Menezes D, et al. Ketones and lactate “fuel” tumor growth and metastasis Evidence that epithelial cancer cells use oxidative mitochondrial metabolism. *Cell Cycle*. 2010;9(17):3506–3514.
66. Gromov P, Espinoza JA, Talman ML, et al. FABP7 and HMGCS2 are novel protein markers for apocrine differentiation categorizing apocrine carcinoma of the breast. *PLoS One*. 2014;9(11):e112024.
67. Soong R, Shah N, Peh BK, et al. The expression of RUNX3 in colorectal cancer is associated with disease stage and patient outcome. *Brit J Cancer*. 2009;100(5):676–679.
68. Voon DCC, Wang HJ, Koo JKW, et al. Runx3 protects gastric epithelial cells against epithelial-mesenchymal transition-induced cellular plasticity and tumorigenicity. *Stem Cells*. 2012;30(10):2088–2099.
69. Hardie DG, Ross FA, Hawley SA. AMPK: a nutrient and energy sensor that maintains energy homeostasis. *Nat Rev Mol Cell Biol*. 2012;13(4):251–262.
70. Danielsen SA, Eide PW, Nesbakken A, Guren T, Leithe E, Lothe RA. Portrait of the PI3K/AKT pathway in colorectal cancer. *Bba-Rev Cancer*. 2015;1855(1):104–121.
71. Hahn-Windgassen A, Nogueira V, Chen CC, Skeen JE, Sonenberg N, Hay N. Akt activates the mammalian target of rapamycin by regulating cellular ATP level and AMPK activity. *J Biol Chem*. 2005;280(37):32081–32089.
72. Porstmann T, Santos CR, Griffiths B, et al. SREBP activity is regulated by mTORC1 and contributes to Akt-dependent cell growth. *Cell Metabol*. 2008;8(3):224–236.
73. Rappa G, Fargeas CA, Le TT, Corbeil D, Lorico A. Letter to the editor: an intriguing relationship between lipid droplets, cholesterol-binding protein CD133 and Wnt/beta-catenin signaling pathway in carcinogenesis. *Stem Cells*. 2015;33(4):1366–1370.
74. Han CC, Wei SH, He F, et al. The regulation of lipid deposition by insulin in goose liver cells is mediated by the PI3K-AKT-mTOR signaling pathway. *PLoS One*. 2015;10(5).
75. Vereshchagina N, Wilson C. Cytoplasmic activated protein kinase Akt regulates lipid-droplet accumulation in Drosophila nurse cells. *Development*. 2006;133(23):4731–4735.
76. van Duijnhoven FJB, Bueno-De-Mesquita HB, Calligaro M, et al. Blood lipid and lipoprotein concentrations and colorectal cancer risk in the European prospective investigation into cancer and nutrition. *Gut*. 2011;60(8):1094–1102.
77. Wang B, Rong X, Palladino END, et al. Phospholipid remodeling and cholesterol availability regulate intestinal stemness and tumorigenesis. *Cell Stem Cell*. 2018;22(2):206.
78. Jain MK, Ridker PM. Anti-inflammatory effects of statins: clinical evidence and basic mechanisms. *Nat Rev Drug Discov*. 2005;4(12):977–987.
79. Gonzalez PS, O’Prey J, Cardaci S, et al. Mannose impairs tumour growth and enhances chemotherapy. *Nature*. 2018;563(7733):719.
80. Violi F, Carnevale R, Pastori D, Pignatelli P. Antioxidant and antiplatelet effects of atorvastatin by Nox2 inhibition. *Trends Cardiovasc Med*. 2014;24(4):142–148.